ARPHA Preprints

PREPRINT

Author-formatted, not peer-reviewed document posted on 25/11/2024

DOI: https://doi.org/10.3897/arphapreprints.e142537

Mitochondrial genomes from fungal the entomopathogenic *Moelleriella* genus reveals evolutionary history, intron dynamics and phylogeny

Xiong Chengjie Xiong, Yongsheng Lin, Nemat O. Keyhani, Junya Shang, Yuchen Mao, Jiao Yang, Minhai Zheng, Lixia Yang, Huili Pu, Longbing Lin, Taicang Mu, Mengjia Zhu, Ziyi Wu, Zhenxing Qiu, Wen Xiong, Xiayu Guan, Junzhi Qiu

 DOI: https://doi.org/10.3897/arphapreprints.e142537

Mitochondrial genomes from fungal the entomopathogenic *Moelleriella* genus reveals evolutionary history, intron dynamics and phylogeny

Chenjie Xiong[1], Yongsheng Lin[1], Nemat O. Keyhani[2], Junya Shang[1], Yuchen Mao[1], Jiao Yang[1], Minhai Zheng[1], Lixia Yang[1], Huili Pu[1], Longbing Lin[1], Taicang Mu[1], Mengjia Zhu[1], Ziyi Wu[1], Zhenxing Qiu[3], Wen Xiong[4], Xiayu Guan[5]*, Junzhi Qiu[1]*

[1] State Key Laboratory of Ecological Pest Control for Fujian and Taiwan Crops, College of Life Sciences, Fujian Agriculture and Forestry University, Fuzhou, Fujian 350002, China

[2] Department of Biological Sciences, University of Illinois, Chicago 60607, USA

[3] Fuzhou Technology and Business University, Fuzhou, Fujian 350715, China

[4] Forestry Diseases and Pests Control Station of Yongding District of Longyan City, Yongding, Fujian 364100, China

[5] College of Horticulture, Key Laboratory of Ministry of Education for Genetics, Breeding and Multiple Utilization of Crops, Fujian Agriculture and Forestry University, Fuzhou, Fujian 350002, China

*Correspondence:

Xiayu Guan

gxy302@126.com

Junzhi Qiu

junzhiqiu@126.com

Abstract

Members of the *Moelleriella* (Hypocreales, Clavicipitaceae) genera are insect pathogens with specificity for scale insects and whiteflies. However, no mitochondrial genomes are available for these fungi. Here, we assembled seven mitogenomes from *M. zhongdongii*, *M. libera*, *M. raciborskii*, *M. gracilispora*, *M. oxystoma*, *Moelleriella* sp. CGMCC 3.18909 and *Moelleriella* sp. CGMCC 3.18913, which varied from 40.8 to 95.7 Kb. Synteny and codon usage bias was relatively conserved; with the mitochondrial gene arrangement completely homologous to the gene order of 16 other species within the Hypocreales. However, extensive intron polymorphism exists between *Moelleriella* species. Evolutionary analyses revealed that all 15 core protein coding genes had ka/ks < 1, indicating purifying selection pressure. Sequence variation within the mitochondrial ribosome protein S3 (*rps3*) gene showed the largest genetic distance with the NADH dehydrogenase subunit 4L (*nad4L*) showing the smallest. Comparative mitogenomic analyses showed that introns were the main factor contributing to the size variation of *Moelleriella* and more widely in Hypocreales mitogenomes. Phylogenetic analyses indicate that the seven *Moelleriella* species examined form a well-supported clade, most closely related to *Hypocrella*. These data present the first mitogenome from *Moelleriella* and further advance research into the taxonomy, origin, evolution,

and genomics of *Moelleriella*.

Keywords: *Moelleriella*, Mitogenome, insect pathogen, phylogeny analysis, Hypocreales, Clavicipitaceae

Introduction

The genus *Moelleriella* belongs to Ascomycota, Sordariomycetes, Hypocreales, Clavicipitaceae, which was established by Bresadola in 1896 to accommodate *M. sulphurea* type species (Chaverri et al., 2008). The genus *Moelleriella* is commonly parasitic on scale insects and whiteflies and currently comprises 52 species. The genus is characterised by brightly coloured ascospores (mainly orange), pyriform to subglobose ascospores, cylindrical ascospores, filiform multiseptate ascospores that disarticulate at the septa within the ascus and aschersonia-like anamorphs with fusoid conidia (Isaka et al., 2009; Khonsanit et al., 2021; Wang et al., 2024). *Moelleriella* is predominantly found in the tropics, with several species isolated from the subtropics, and shows an Old World (OW)/New World (NW) disjunction in distribution (Aylor et al., 1999; Agrawal et al., 2016). In addition, geographically restricted species have been reported for some members of *Moelleriella* (Oborník et al., 2000). As sensitivity to ultraviolet light, solar radiation and temperature are important

factors known to affect the survival of entomopathogenic fungal spores, as well as of hosts such as whiteflies, most *Moelleriella*-infected specimen are found on the underside of forest foliage, *i.e.*, leaves, and under conditions of high relative humidity (Brancini et al., 2022; Seib et al., 2023; Bohatá et al., 2024) . Traditionally, *Moelleriella* species and members of closely related genera have been classified on the basis of morphological differences, and although the majority of *Moelleriella* species can apparently be cultured on standard media, a comprehensive substrate allowing for growth of all species has not been reported, and neither have fungal sexual structures been observed during growth on artificial media (Chaverri et al., 2005; Zhu and Zhuang, 2015). *Moelleriella* species can most often be reliably distinguished by observing the characteristics of spores, coupled to molecular taxonomic analyses of the sequences of various loci, *e.g.*, *LSU*, *EF1-α*, and *RPB1*. The genus *Moelleriella* is currently divided into the “effuse” “globose” branches based on DNA sequence data that correlated with stromatal morphology, with each branch containing 13 species (Chaverri et al., 2008; Yang et al., 2023). However, lack of more comprehensive molecular data and heterogeneity continue to be important obstacles in the study of phylogenetic analyses of *Moelleriella* species, as well as our understanding of their host specificity and distribution.

Scale insects (Coccidae and Lecaniidae, Homoptera) and whiteflies are major pests and target a wide variety of host plants. In particular, they act as

important vectors for the transmission of a wide range of plant viruses and are often difficult to control. Species of *Moelleriella* have been recognized as pathogens of scale insects/whiteflies by modern naturalists in the late 19th century (Mongkolsamrit et al., 2011; Wang et al., 2014) , with *M. libera* (anamorph *A. aleyrodis*) one of the first species used for whitefly control in Eastern Europe and Asia (Qiu et al., 2013; Ausique et al., 2017) . Further studies have showed *Moelleriella* species to be promising for pest biological control, including as a resource for green agriculture development and as part of Integrated Pest Management (IPM) practices. However, significant obstacles include the observation that most species of *Moelleriella* produce few spores in artificial media, making them difficult to produce on a large scale (Campos-Esquivel et al., 2022) . Even with such current limitations, the metabolites of *Molleriella* species have been shown to possess a variety of activities of biopharmaceutical interest, including compounds that display anti-proliferative, anti-malarial and anti-bacterial/fungal activities (Guo et al., 2015; Sadorn et al., 2020; Aragão et al., 2024). Knowledge concerning genetic features of *Molleriella* species, can therefore help in cultivation, bioprospecting, and pest control application.

Mitochondria contain their own genomes and are double-membrane organelles that provide energy for normal life activities in eukaryotes and are involved in signalling, genetic evolution and other processes (Gray et al., 2001; Murphy et al., 2009; Muñoz-Gómez et al., 2017). Genetic variation in

the mitochondrial genome due to its matrilineal inheritance properties, can be used to examine diversity and evolutionary processes (Basse 2010; Wang et al., 2018; Li et al., 2022; Song et al., 2024) . Although the mitochondrial genomes of fungal genera vary significantly, most fungi typically contain 15 conserved protein-coding genes (PCGs) which include: *atp6*, *atp8*, *atp9*, *cob*, *cox1*, *cox2*, *cox3*, *nad1*, *nad2*, *nad3*, *nad4*, *nad4L*, *nad5*, *nad6* and *rps3* (Li et al., 2019; Castrillo et al., 2023) . In addition to these conserved genes, two ribosomal RNAs, *rns*, *rnl* and tRNAs also occur in fungal mitochondrial genomes (Wu et al., 2021; Zubaer et al., 2021). To date, there are no reports on the mitochondrial genomes of *Moelleriella* species, and here we report on the sequence, assembly and annotation of the mitogenomes of seven *Moelleriella* species. These genomes were analysed with respect to codon preference, intron dynamics, gene homology, and extrapolated to evolutionary analyses of the core PCGs within Hypocreales. Furthermore, a phylogeny based on the mitogenome dataset was sued to clarify the evolutionary position of *Moelleriella* in Hypocreales. Our results fill gaps in the mitochondrial genomic information of *Moelleriella*, and provide references data for molecular analyses on the origin, evolution, and diversity within *Moelleriella*.

Materials and methods

Sample collection and DNA extraction

The specimens were collected from the provinces of Fujian, Jiangxi and

Zhejiang, and the samples were kept dry after collection. One to two fresh ascospores were selected and dispersed as a spore suspension in sterile dH_2O on an ultra-clean workbench, and uniformly spread on the PDA plate. Isolates were single colony purified or allowed to grow as a mycelium after which the edge was used for subculturing. Once purified, growing mycelia were maintained in 30% glycerol and stored at -80°C. A total of seven *Moelleriella* species were used for molecular multilocus nucleotide sequencing. Target loci included the *LSU*, *RPB1* and *EF-1α* sequences which were amplified and analysed as described (Mu et al., 2024; Zhao et al., 2024). In addition, morphological characteristic for each isolate was determined. Total DNA was extracted using the Fungal DNA Mini Kit (OMEGA-D3390, Feiyang Biological Engineering Corporation, Guangzhou, China). The concentration and purity of each sample was confirmed via spectroscopic analyses (Nanodrop, Thermo Fisher Scientific, USA).

Mitogenome sequencing and assembly

High-quality genomic DNA was utilized for the construction of sequencing libraries. The libraries were sequenced using the Illumina HiSeq platform with a 2×150 double-end sequencing strategy. Raw sequences obtained were quality assessed and filtered to obtain clean sequences using the FastaP v0.20.0 (Chen 2023) , and used Kraken2 v2.1.3 to identify mitochondrial sequences in the sequencing data (Breitwieser et al., 2018) . Assembled

filtered sequences were analysed using SPAdes v3.14.1 and NOVO Plasty was used to validate assembly of the mitogenome sequences (Bankevich et al., 2012; Dierckxsens et al., 2017).

Annotation of mitogenomes

The annotation of protein-coding genes (PCGs), introns, rRNA genes and tRNA genes of the mitogenome was conducted using the MFannot and MITOS2 (Bernt et al., 2013; Valach et al., 2014), rRNA and tRNA sequence analyses were also examined using RNAweasel (https://github.com/BFL-lab/RNAweasel) and tRNAscan-SE v2.00 for validation (Lowe and Chan, 2016). Subsequently, the NCBI Open Reading Frame (ORF) Finder (https://www.ncbi.n- lm.nih.gov/orffinder) was employed to predict ORFs in the assembled mitochondrial genomes, with analyses followed by functional annotation using Blastn and BlastP (Bleasby and Wootton, 1990). Intron-exon boundaries were detected using exonerate v2.2 (Slater and Birney, 2005). All annotation results were manually corrected as needed. Graphical maps of the assembled mitogenomes were drawn using OGDraw v1.3.1(Greiner et al., 2019).

Sequence analysis

The base compositions of the mitogenomes were calculated using the MEGA 11 v11.0.13 (https://megasoftware.net/). GC skew and AT skew were

calculated according to the following formulas: AT skew = [A − T]/[A + T], and GC skew = [G − C]/[G + C] (Wang et al., 2017). RSCU values were determined using Condon W (https://sourceforge.net/projects/codonw/). A total of 15 core protein coding genes were individually aligned using MAFFT v7.11 from 27 mitogenomes (7 determined here, and 20 from the NCBI database) (Katoh et al., 2002). Nonsynonymous substitution rates (Ka) and synonymous substitution rates (Ks) of the core PCGs were calculated using the DnaSP v5.1.0 (Librado and Rozas, 2009). MEGA11 v11.0.13 software, using the Kimura-2-parameter (K2P) substitution model, was employed to detect paired genetic distances between the 15 core PCGs. BLASTn (e-value 10^{-10}) was also used to compare the *Moelleriella* mitogenomes and to detect the presence of any large segments of intragenomic duplications within their genomes (Chen et al., 2015). Tandem repeats were identified using the Tandem Repeats Finder (Benson, 1999).

Comparative analyses of mitogenomes and intron analysis

The *Moelleriella* mitogenomes were compared using BLASTn (e-value 10^{-6}), with homology analyses utilising TBtools (Chen et al., 2023). The length and compositional distribution of the mitogenomes of 27 species from the Hypocreales was examined using ggplot2 v.4.3.2 (https://github.com/tidyverse/ggplot2), and correlations between mitogenome size and the six components (core PCGs, RNA regions, intergenic

regions, intronic regions, homing endonuclease genes (HEGs) and un_orf) were calculated. Intron dynamics analyses were performed as previously described (Ji et al., 2023). To determine insertion positions of introns, comparisons were conducted using MAFFT v.7.11, based on genetic code 4 and codons. The mitogenome from *M. gracilispora* was used as a reference to describe intron insertion positions. A total of three introns insertion positions differences between species were still considered to have the same overall intron insertion distribution.

Mitochondrial phylogenetic analysis

The mitogenomes of 94 Ascomycota species were downloaded from the NCBI database and a phylogenetic tree was constructed based on the combined dataset (14 conserved protein coding genes) to determine phylogenetic relationships. *Pleurotus ostreatus* from the class Agaricomycetes was used as the out group. The 14 fungal core PCGs were aligned using the MAFFT v.7.11, followed by manual adjustments in MEGA11 v11.0.13. Subsequently, the PCGs were merged into a combined dataset using PhyloSuite v1.2.3 (Xiang et al., 2023) . Phylogenetic analyses were conducted based on both maximum likelihood (ML) and Bayesian inference (BI) methods. ML analysis was performed using RaxML-HPC2 on XSEDE v.8.2.12 via the CIPRES Science Gateway portal, while BI analysis was carried out by MrBayes on XSEDE v.3.2.7a(https://www.phylo.org/). The best evolutionary models for

individual partitions were determined on the basis of MrModeltest v.2.3.MCMC chains were executed for 160,000 generations with a sampling frequency of 100 generations. A burn-in fraction of 0.25 was implemented, and posterior probabilities (PP) were inferred from the resulting trees. The consensus tree was constructed using FigTreev.1.4.4 (http://tree.bio.ed.ac.uk/software/figtree/). Newly generated sequences from this study have been deposited in GenBank. Branches showing ML bootstrap support values ($\geqslant$ 70) and Bayesian posterior probability ($\geqslant$ 0.90) were considered significantly supported.

Data availability

The complete mitogenomes of the seven *Moelleriella* species were deposited in the GenBank database under the accession numbers PQ367224–PQ367230.

Results

Characterization of the seven Moelleriella mitogenomes

The circular mitochondrial genomes of seven *Moelleriella* species were determined as follows: 57023 bp for *M. zhongdongii*, 40823 bp for *M. libera,* 45471 bp for *M. raciborskii*, 79556 bp for *M. gracilispora*, 95666 bp for *M.oxystoma*, 5389 bp for *Moelleriella* sp.C9(*Moelleriella* sp. CGMCC3.18909, unpublished data), and 54896 bp for *Moelleriella* sp.C3(*Moelleriella* sp. CGMCC3.18913, unpublished data)(Figure1). The highest GC content was

observed in *M. raciborskii* (28.20%), while the lowest was seen in *Moelleriella* sp.C3 (26.10%). The average GC content was 27.10%. GC-skew values in the mitogenomes were from 0.0943 to 0.1128, and AT-skew values were from 0.0291 to 0.0572, the AT and GC skews were found to be positive for all seven mitogenomes. In total, the number of protein-coding genes present in *Moelleriella* mitogenome determined ranged from 18 to 26 (Table S1). Each mitogenome encoded 15 core PCGs (*atp*6, *atp*8, *atp*9, *cob*, *cox*1-3, *nad*1-6, *rps*3), two ribosomal RNAs (*rns* and *rnl*), and tRNA gene numbers ranging from 25 to 27 (Fig. 1, Table S2).

Moelleriella oxystoma was found to contain 12 uncharacterized open reading frames (un_ORFs), whereas *M. raciborskii* had only one, with other species ranging from 5-12. The number and distribution of introns exhibited significant variation. Intronic analyses revealed that *M. gracilispora* and *M. oxystoma*, contained more introns than the other species examined, and that these were mainly distributed in the *cob*, *cox*1, *cox*3, *nad*1 and *rnl* genes. *M. libera* had the fewest introns, which were mainly distributed in the *cob*, *cox*2-3, *nad*1, *nad*5, and *rnl* genes. Variable numbers of intronic ORFs encoding GIY-YIG and LAGLIDADG homing endonucleases were identified in the mitogenomes (Table S2). In terms of sequence composition, PCGs were consisted of the largest percentage (average =34.78%), while RNA regions constituted an average of 11.33% of the total sequence (Table S3).

Codon usage analysis

The codon usage patterns in different Hypocreales mitogenomes were analysed. The *cox*1 gene in 23 Hypocreales mitogenomes utilized ATG as its start codon, 3 others used TTG, and *Pleurocordyceps sinensis* used ATA. Most core PCGs in the 27 Hypocreales mitogenomes used ATG as start codons, although the *cob* gene of *Stachybotrys chlorohalonata* and *Stachybotrys chartarum* uesd GTG as start codons. In addition, the *cox*2 gene of *Moelleriella* sp.C3, the *cox*3 gene of *S.chlorohalonata* and *S. chartarum,* and the *nad*3 gene of *M. zhongdongii*, *M. oxystoma* and *Moelleriella* sp.C9 used TTG as their start codon. Two different stop codons were found in the mitogenomes of the 27 Hypocreales species examined. These include TAA, which was detected in 15 genes, and TAG found in seven genes (*atp*9, *cob*, *nad*1, *nad*3, *nad*5, *nad*6, *rps*3)(Table S4). Codon usage analysis indicated that the most commonly used codons in the *Moelleriella* mitogenomes were UUA (leucine; Leu), followed by AGA (arginine; Arg) (Fig. 2A). Furthermore, codon usage bias in *Moelleriella* was essentially identical to other Hypocreales species.

Repetitive sequence analysis

The *Moelleriella* mitogenomes analysed contained 2-16 repeat regions. The size of these sequences varied from 35 to 405 bp, with the largest repeat identified in *M. oxystoma* in the *nad*2 gene. The second largest repeat (284 bp) region was found in the *M. gracilispora cox*2 gene. Pairwise nucleotide identities of

the repeater sequences between the *Moelleriella* mitogenomes ranged from 76-100%, and intra-genomic repeats accounted for 1.02%, 0.32%, 0.38, 3.53%, 3.06%, 1.91% and 0.37% of the mitogenomes of *M. zhongdongii, M. libera, M. raciborskii, M. gracilispora, M. oxystoma, Moelleriella* sp. C9 and *Moelleriella* sp.C3, respectively (Table S6).

A total of 68 tandem repeats were found in the *Moelleriella* mitogenomes, with the number of repeats ranging from 4 to 14. The longest tandem repeat was found in *M. raciborskii* (136 bp). All of the tandem repeats were duplicated 1-2 times in the seven *Moelleriella* mitogenomes. The proportions of tandem repeat in *M. oxystoma, M. gracilispora, Moelleriella* sp.C3*, Moelleriella* sp.C9*, M.raciborskii, M. libera,* and *M. zhongdongii* were 0.29%, 0.51%, 0.74%, 0.77%, 0.81%, 1.22% and 1.32%, of the total mitogenome, respectively (Table S7).

Genetic distance and evolutionary rates of core PCGs

Within the 15 core PCGs, the *rps*3 gene had the highest median Kimura-2-parameter distance (K2P) genetic distance in the 27 Hypocreales species dataset used, followed by the *nad*6 and *atp*6 genes, indicating that these genes diverged early and have accumulated the highest level of change (mutations) as compared to the other mitochondrial PCGs. The *nad*4L gene has the lowest median K2P distance, indicating the lowest degree of change (high conservation). These findings were furthers supported by analyses which showed that the *rps*3 and *nad6* genes had the highest mean number of

nonsynonymous substitutions per nonsynonymous site (Ka values), and the *nad*4L gene the lowest. The *nad*3 gene had the highest synonymous substitution rate (Ks), while the *rps*3 gene had the lowest Ks value (Fig. 3, Table S8). The Ka/Ks values of the 15 core PCGs were all well below 1, indicating that these genes have undergone strong purifying selection during evolution.

Intron dynamics in Moelleriella mitogenomes

Intron numbers varied: *M. zhongdongii*(17), *M. libera*(9), *M. raciborskii*(13), *M.gracilispora*(34), *M. oxystoma*(33), *Moelleriella* sp.C9(16) and *Moelleriella* sp.C3 (16), and where dispersed in 13 genes: *atp*6, *atp*9, *cob*, *cox*1, *cox*2, *cox*3, *nad*1, *nad*2, *nad*4L, *nad*5, *nad*6, *rnl* and *rns* (Fig. 4), with intron gain and loss seen. Introns were classified into intron position sets (IPSs) based on insertion positions in *M. gracilispora* genes and common introns were defined as those occurring in the same IPS across the *Moelleriella* mitogenomes examined.

These data revealed a total of 138 IPSs (Figure 4A), of which 13 were common among the *Moelleriella* species, with each *Moelleriella* species also containing unique introns. The *cox*1 gene had the highest number of introns, followed by the *rnl* and *cob* genes. In *Moelleriella* species, most of the introns in the *cox*1 gene were conserved, but only one intron in the *cob* gene was conserved (*cob*-393). Highly conserved introns were also found in the *nad*1, *cox*2, *cox*3 and *nad*5 genes. Only *M. oxystoma* contained introns in the *nad*6

and *nad*2 genes, the presence of introns in the *rns* gene was only seen in *M. raciborskii* and *M.gracilispora*. Contrary to PCGs, non-coding genes (e.g., *rnl*) exhibited lower intron insertion position conservation (Figure 4A). Except for *M. raciborskii*, *M.libera* and *M. zhongdongii*, the intron lengths of the remaining four *Moelleriella* species showed a clear unimodal distribution, *M. raciborskii* showed a bimodal distribution, whereas *M. libera* and *M. zhongdongii* showed a three-peaked distribution (Figure 4B). Intron lengths of all *Moelleriella* species were enriched in the 1000-2000 bp length region. Length distributions of common introns and species-specific introns showed no significant differences (Figure 4C). In addition, in most *Moelleriella* species examined, there were more introns in the mitogenome located between codons (phase 0) than between the first and second bases within codons (phase 1) or between the second and third bases (phase 2) (Figure 4D). The number of introns in phase 1 was comparable to that in phase 2, but in *M. raciborskii* and *M. libera*, the number of introns in phase 1 was less than that in phase 2. *M. zhongdongii* showed a codon phase distribution with almost equal numbers in each category.

Comparative analysis of Hypocreales mitogenomes

A comparative analysis of the mitogenomes of 27 species of Hypocreales, including seven species of *Moelleriella*, was conducted. The size of the genome exhibited considerable variability, ranging from 23794 bp (*Orbiocrella petchii*)

to 99850 bp (*Fusarium ussurianum*), with a mean value of 44953 bp (Fig. 5, Table S1). Furthermore, the proportion of the five fractions (un_ORFs, intronic regions, intergenic regions, RNA regions, and core PCGs) varies between different species. Core PCGs and RNA regions account for more than 60% of the mitogenome in fungi such as *Memnoniella echinata*, *Purpureocillium takamizusanense* and *Cordyceps militaris,* and only 1/3 or less in other species. The proportion of intergenic regions ranged from 7.14% to 29.08% across different species, meanwhile, un_ORFs percentages ranged from 5% to 30% across species. Conversely, in fungi such as *Samsoniella hepiali*, *Cordyceps militaris*, and *Orbiocrella petchii*, there is no un_orf (Figure 5, Table S1).

Furthermore, we investigated the potential correlation between mitogenome size and its content. Our findings surface that significant positive correlations were found between mitogenomic lengths and intergenic regions ($R = 0.759$, $p = 3.3 \times 10^{-9}$), HEGs ($R = 0.941$, $p = 1.3 \times 10^{-10}$), intronic regions ($R = 0.961$, $p = 3.8 \times 10^{-19}$), and un_ORF sequences ($R = 0.702$, $p = 2.1 \times 10^{-6}$), which has been demonstrated that they exert a significant influence on the variability observed in mitogenomic size (Fig.6C-F). However, RNA regions and core PCG lengths displayed no notable correlation with mitogenomic size ($R = 0.017$, $p = 0.51$, $R = 0.199$, $p = 0.02$)(Fig.6A, B). The observed differences in mitogenome composition across 27 Hypocreales species could be attributed to several factors, including repetitive sequence transfers and gain/loss events of introns and un_ORFs. These mechanisms may

explain the observed variations in mitogenome length among these species.

Gene arrangement in the mitogenome

We compared the arrangements of 15 core PCGs and 2 rRNAs in the 27 Hypocreales mitogenomes and found that 23 members exhibited identical gene arrangement, with isolates within *Stachybotrys*, *Metacordyceps* and *Clonostachys* showing differences and following the gene order: *cox*1, *nad*1, *nad*4, *atp*8, *atp*6, *rns*, *cox*3, *nad*6, *rnl*, *rps*3, *nad*2, *nad*3, *atp*9, *cox*2, *nad*4L, *nad*5, *cob*. *Stachybotrys* and *Metacordyceps* have their *nad*2 and *nad*3 genes positioned between the *cox*1 and *atp*9 genes rather than between the *rps*3and *atp*9 genes as seen in most Hypocreales mitogenomes analyzed, with *Clonostachys* having the *cox*2 gene between the *nad*4 and *atp*8 genes (Fig. 7). In general, the mitogenomes of Hypocreales exhibit a high degree of conservation.

Phylogenetic and synteny analysis

To reconstruct the evolutionary lineage of the analysed mitogenomes, phylogenetic trees were constructed using two phylogenetic inference methods, Bayesian inference (BI) and maximum likelihood inference (ML), based on the DNA sequences of the 14 conserved mitochondrial protein-coding genes (PCGs) using a combined dataset from 95 different species from eight orders (Table S9). Identical tree topologies were obtained using the two phylogenetic inference methods, with *Pleurotus ostreatus* used as

the outgroup. All the major clades were well-supported in the phylogenetic tree (BPP ≥ 0.90;BS =100), and those of the same genus grouped in the same branch and show similar or consistent characteristics in terms of GC content and gene conservation(Fig.8). This analysis also revealed a close evolutionary relationship between *Moelleriella* and *Hypocrella*. To further assess the relationship between the mitogenomes of *Moelleriella* and its closest relatives, homologous genes were compared using BLASTN. These analyses indicated a considerable number of homologous co-linear fragments within *Moelleriella* (Fig. 9, Table S10), with the longest between *Moelleriella* sp.C3 and *Moelleriella* sp.C9 (6737bp). The highest number of homologous collinear fragments was observed in *Moelleriella* sp.C3 and *M. gracilispora*, with lower levels seen between *Moelleriella* and its close relative, *H. discoidea*, with the latter showing extensive rearrangements.

Discussion

The mitogenome sizes of seven *Moelleriella* species ranged from 40,828 to 95,666 bp, with an average size of 61,038 bp. Previous studies have shown that the main factors contributing to variations in the size of fungal mitochondrial genomes are varying numbers of introns, the accumulation and distribution of repetitive sequences, and the dynamics of intergenic regions (Ma et al., 2022) . Our data indicate that intron insertions were the main cause of mitogenome size variation between *Moelleriella* species, and that

the number of introns was proportional to genome size. More broadly, mitogenomes within the Hypocreales species varied considerably, ranging from 23754 to 99850 bp. Correlation analysis revealed that the sizes of the un_ORFs, HEGs, intronic regions, and intergenic regions contributed to mitogenome length variation (correlation coefficients > 0.7), which suggest significant intron drift and the acquisition/loss, particularly of un_ORFs, in Hypocreale. Furthermore, GC skew and AT skew varied considerably among the 27 species examined, with most species having positive GC and AT skew, indicating someinter-genera differences.

As with almost all fungal mitogenomes characterized thus far, all seven *Moelleriella* species described herein, contained a core set of PCGs that play an important role in cellular energy metabolism and functional maintenance (Allen, 2015). Some differences in length, GC content, and base composition of the core PCGs were noted, and the evolutionary trajectory of these genes display different levels of change and positive/purifying selection (Huang et al., 2024). Codon usage is often linked to gene expression levels and can be used to gain evolutionary insight into species relatedness. We found almost identical codon preferences in the mitogenomes of the seven *Moelleriella* species characterized, with some variation in use of start and stop codons for the core PCGs. In addition, several non-conserved PCGs of unknown function were identified, suggesting unknown functions encoded therein and gene gain/loss in specific lineages.

Introns are prevalent in fungal mitochondrial genomes and are mainly divided into groups I and II, with the *cox*1 gene usually containing the largest number of introns, and intron polymorphisms affect the size and evolution of fungal mitotic genomes (Férandon et al., 2010; Stone et al., 2018; Li et al., 2023). IPS analyses were used to delineate and compare the location of intron insertions. These analyses revealed that intron insertion sites exhibit frequent gain/loss dynamics, and none of the introns were shared by all seven *Moelleriella* species examined. These data are similar to what has been observed in *Cordyceps* and other fungi (Zhang et al., 2013). Approximately 5-10% of group I introns typically carry HEGs that can potentially act as mobile genetic elements (Hedberg and Johansen, 2013) . A total of 138 introns were identified in our *Moelleriella* analysis, most of which were group I with HEGs. While it is unclear which may be “active”, these findings may account for the diversity of intron insertion positions found. In addition, introns were evenly distributed in the *Moelleriella* mitogenomes, and intron positions in different species were most prevalent between codons ("phase 0"), similar to what has been commonly described (Nielsen and Wernersson, 2016) . Overall, the fact that the *Moelleriella* species examined share a small number of intron insertion positions suggests loss of ancestral introns and large changes in intron insertion positions during evolution.

Compared to nuclear genomes, mitochondrial genomes typically evolve at faster rates and are more prone to accumulating mutations, which can increase

their analytic utility for monitoring evolutionary changes during species differentiation. One aspect of this is the order of mitochondrial genes, which can undergo rearrangement, can readily be seen in genome alignment analyses, and hence has been used an important reference for reconstructing the evolutionary relationships (Li et al., 2018, 2021). However, mechanisms of rearrangement of fungal mitochondrial genomes may be more intricate than previously thought, and some caution should be taken in deriving conclusions (Zheng et al., 2018). Despite gene rearrangements being widespread in fungi, our study found that the *Moelleriella* mitogenomes have a consistent gene arrangement which is generally conserved throughout the Hypocreales. Different gene arrangements were found only in *Stachybotrys chartarum*, *Stachybotrys chlorohalonata* and *Metacordyceps chlamydosporia*, consistent with previous findings (Xia et al., 2016) . Recent studies have shown that the mitogenomes of Hypocreales species display six different patterns of gene arrangement and five different patterns of *nad*2/*nad*3 connectivity, most of which are rare, and that the rare patterns are restricted to a few fungal species or groups of fungi (Xia et al., 2016). Our data do show however, important rearrangements in the *Moelleriella* mitogenomes, consisting of mostly small homologous fragments, with many homologous co-linear genomic blocks shared with close relatives, while the 15 core PCGs and 2 rRNA genes were completely conserved. These data suggest *Moelleriella* species may have undergone important changes during evolution centered around mechanisms

that cause frequent short fragment rearrangements, with certain regions more prone to recombination (“hot spots”), especially those near repetitive sequences or gene spacer regions. It is well recognized that the mitochondrial genome is independent of the nuclear genome and has characteristics of more rapid evolution. Mitochondrial genes have been used as reference “molecular markers”, as tools for studying the phylogenetic placement and evolution of fungi(Chen et al., 2019).

Moelleriella species have important potential for insect biological control especially against whitefly and scale insect pests (Chaverri et al., 2008). Our data and phylogenetic analysis of *Moelleriella*, using the mitochondrial genome, can allow for the accurate classification of this genus. Based on the combined mitochondrial gene set and two phylogenetic inference methods, we obtained a strongly supported phylogenetic analysis of 94 related species within the Ascomycota. Our results indicate strong support for the seven identified *Moelleriella* species clustered together within a distinct clade with a high level of support, with *Hypocrella* the closest relative to *Moelleriella*. Interestingly, *Hypocrella* (which are also entomopathogens) appear to be specific to true soft scale insects, being restricted to members of the Aleyrodidae(whiteflies)and Coccidae (family of soft scales insects within the superfamily Coccoidea).

Conclusions

In this study, we assembled and annotated seven mitogenomes from the

species within the genus *Moelleriella* from which no information is currently available. The mitogenomes differed in size, and comparative analyses with 27 Hypocreales species showed that un_ORFs, HEGs, and intronic and intergenic regions were the key factors influencing genome size, with the greatest contribution to variation from intronic regions. The codon usage preferences of the *Moelleriella* species were conserved, and the core PCGs within Hypocreales showed varying degrees of selective purification pressure and show different rates of change (evolution). Intron insertion sites varied among the *Moelleriella* species, suggesting intron gain/loss events during speciation. The order (arrangement) of the PCGs was highly conserved among Hypocreales species, however, different some variation was observed in *Stachybotrys* and *Clonostachys*. Finally, a phylogeny based on mitochondrial gene assemblies and two phylogenetic inference methods reveals the evolutionary position of *Moelleriella* species in the Hypocreales. Our data report the first mitogenomes of *Moelleriella* providing valuable information on the genetics, evolution and genomics of this genus.

Supplementary Information

Supplementary data to this article can be found online at GenBank: https:// www. ncbi. nlm. nih. gov/ genbank/.

Author contributions

CX: Conceptualization, Resources, Data curation, Formal analysis, Investigation, Writing – original draft. **YL, HP:** Resources, Formal analysis. **JS, YM, ZW:** Data curation, Investigation, Software. **NK:** Writing – review & editing. **JY, MZ:** Resources, Writing – review & editing. **LY:** Investigation, Writing – review & editing. **TM:** Resources, Writing – review & editing. **LL:** Software, Writing – review & editing. **MZ:** Resources, Writing – review & editing. **ZQ, WX:** Resources, Writing – review & editing. **XG:** Conceptualization, Resources, Writing – review & editing. **JQ:** Conceptualization, Resources, Supervision, Writing – review & editing, Funding acquisition.

Funding

This research was funded by the National Natural Science Foundation of China (No. 32270029, U1803232, 31670026), the National Key R & D Program of China (No. 2017YFE0122000), a Social Service Team Support Program Project (No. 11899170165), Science and Technology Innovation Special Fund (Nos. KFB23084, CXZX2019059S, CXZX2019060G) of Fujian Agriculture and Forestry University, a Fujian Provincial Major Science and Technology Project (No. 2022NZ029017), an Investigation and evaluation of biodiversity in the Jiulong River Basin (No. 082·23259-15), Macrofungal and microbial resource investigation project in Longqishan Nature Reserve (No.

SMLH2024(TP)-JL003#), and an Investigation of macrofungal diversity in Junzifeng National Nature Reserve, Fujian Province (No. Min Qianyu Sanming Recruitment 2024-23).

Availability of data and materials

All data generated or analyzed during this study are included in this published article.

Declarations

Ethics approval and consent to participate

Not applicable.

Adherence to national and international regulations

Not applicable.

Consent for publication

Not applicable.

Competing interests

The authors declare that they have no competing interests.

References

Agrawal Y, Narwani N, Subramanian S (2016) Genome sequence and comparative analysis of clavicipitaceous insect-pathogenic fungus *Aschersonia badia* with *Metarhizium* spp. BMC genomics 17: 367

Allen JF (2015) Why chloroplasts and mitochondria retain their own genomes and genetic systems: Colocation for redox regulation of gene expression. Proc Natl Acad Sci U S A 112(33): 10231–10238

Aragão TMS, dos Santos JVFC, Santos TS, Souto EB, Severino P, Jain S, Mendonça MdC (2024) Scientific-technological analysis and biological aspects of entomopathogenic fungus *Aschersonia*. Sustain Chem Pharm 24: 100562

Ausique JJS, D'Alessandro CP, Conceschi MR, Mascarin GM, Júnior ID (2017) Efficacy of entomopathogenic fungi against adult *Diaphorina citri* from laboratory to field applications. J Pest Sci 90(3): 946–960

Aylor JE, Hyde KD, Jones EBG (1999) Endophytic fungi associated with the temperate palm, *Trachycarpus fortunei*, within and outside its natural geographic range. New Phytol 142(2): 335–346

Bankevich A, Nurk S, Antipov D, Gurevich AA, Dvorkin M, Kulikov AS, Lesin VM, Nikolenko SI, Pham S, Prjibelski AD, Pyshkin AV, Sirotkin AV, Vyahhi N, Tesler G, Alekseyev MA, Pevzner PA (2012) SPAdes: A New Genome Assembly Algorithm and Its Applications to Single-Cell

Sequencing. J Comput Biol 19(5): 455–477

Basse CW (2010) Mitochondrial inheritance in fungi. Curr Opin Microbiol 13(6): 712–719

Benson G (1999) Tandem repeats finder: a program to analyze DNA sequences. Nucleic Acids Res 27(2): 573–580

Bernt M, Donath A, Jühling F, Externbrink F, Florentz C, Fritzsch G, Pütz J, Middendorf M, Stadler PF (2013) MITOS: Improved *de novo* metazoan mitochondrial genome annotation. Mol Phylogenet Evol 69(2): 313–319

Bleasby AJ, Wootton JC (1990) Construction of validated, non-redundant composite protein sequence databases. Protein Eng 3(3): 153–159

Bohatá A, Folorunso EA, Lencová J, Osborne LS, Mraz J (2024) Control of sweet potato whitefly (*Bemisia tabaci*) using entomopathogenic fungi under optimal and suboptimal relative humidity conditions. Pest Manag Sci 80(3): 1065–1075

Brancini GTP, Hallsworth JE, Corrochano LM, Braga GUL (2022) Photobiology of the keystone genus *Metarhizium*. J Photochem Photobiol B 226: 112374

Breitwieser FP, Baker DN, Salzberg SL (2018) KrakenUniq: confident and fast metagenomics classification using unique *k*-mer counts. Genome Biol 19(1): 198

Campos-Esquivel L, Hanson PE, Escudero-Leyva E, Chaverri P (2022) Virulence of native isolates of entomopathogenic fungi (Hypocreales) against the “sweetpotato whitefly” *Bemisia tabaci* (Hemiptera:

Aleyrodidae), including the effects of temperature and fungicides. J Invertebr Pathol 192: 107787

Castrillo ML, Bich GÁ, Amerio NS, Barengo MP, Zapata PD, Saparrat MCN, Villalba LL (2023) *Trichoderma koningiopsis* (Hypocreaceae) has the smallest mitogenome of the genus *Trichoderma*. Front Microbiol 14: 1141087

Chaverri P, Bischoff JF, Liu M, Hodge KT (2005) A new species of *Hypocrella*, *H. macrostroma*, and its phylogenetic relationships to other species with large stromata. Mycol Res 109(11): 1268–1275

Chaverri P, Liu M, Hodge KT (2008) A monograph of the entomopathogenic genera *Hypocrella*, *Moelleriella*, and *Samuelsia* gen. nov. (*Ascomycota*, *Hypocreales*, *Clavicipitaceae*), and their aschersonia-like anamorphs in the Neotropics. Stud Mycol 60: 1–66

Chen C, Li Q, Fu R, Wang J, Xiong C, Fan Z, Hu R, Zhang H, Lu D (2019) Characterization of the mitochondrial genome of the pathogenic fungus *Scytalidium auriculariicola* (Leotiomycetes) and insights into its phylogenetics. Sci Rep 9(1): 17447

Chen C, Wu Y, Li J, Wang X, Zeng Z, Xu J, Liu Y, Feng J, Chen H, He Y, Xia R (2023) TBtools-II: A "one for all, all for one" bioinformatics platform for biological big-data mining. Mol Plant 16(11): 1733–1742

Chen S (2023) Ultrafast one-pass FASTQ data preprocessing, quality control, and deduplication using fastp. iMeta 2(2): e107

Chen Y, Ye W, Zhang Y, Xu Y (2015) High speed BLASTN: an accelerated MegaBLAST search tool. Nucleic Acids Res 43(16): 7762–7768

Dierckxsens N, Mardulyn P, Smits G (2017) NOVOPlasty: de novo assembly of organelle genomes from whole genome data. Nucleic Acids Res 45(4): e18

Férandon C, Moukha S, Callac P, Benedetto JP, Castroviejo M, Barroso G (2010) The *Agaricus bisporus cox1* Gene: The Longest Mitochondrial Gene and the Largest Reservoir of Mitochondrial Group I Introns. PLoS One 5(11): e14048

Gray MW, Burger G, Lang BF (2001) The origin and early evolution of mitochondria. Genome Biol 2(6): REVIEWS1018

Greiner S, Lehwark P, Bock R (2019) OrganellarGenomeDRAW (OGDRAW) version 1.3.1: expanded toolkit for the graphical visualization of organellar genomes. Nucleic Acids Res 47(W1):W59–W64

Guo Q, Dong L, Zang X, Gu Z, He X, Yao L, Cao L, Qiu J, Guan X (2015) A new azaphilone from the entomopathogenic fungus *Hypocrella* sp. Nat Prod Res 29(21): 2000–2006

Hedberg A, Johansen SD (2013) Nuclear group I introns in self-splicing and beyond. Mob DNA 4(1): 17

Huang Y, Wang H, Huo S, Lu J, Norvienyeku J, Miao W, Qin C, Liu W (2024) Comparative Mitogenomics Analysis Revealed Evolutionary Divergence among *Neopestalotiopsis* Species Complex (Fungi: *Xylariales*). Int J Mol Sci 25(6): 3093

Isaka M, Hywel-Jones NL, Sappan M, Mongkolsamrit S, Saidaengkham S (2009) Hopane triterpenes as chemotaxonomic markers for the scale insect pathogens *Hypocrella* s. lat. and *Aschersonia*. Mycol Res 113(4): 491–497

Ji X, Tian Y, Liu W, Lin C, He F, Yang J, Miao W, Li Z (2023) Mitochondrial characteristics of the powdery mildew genus *Erysiphe* revealed an extraordinary evolution in protein-coding genes. Int J Biol Macromol 230: 123153

Katoh K, Misawa K, Kuma K, Miyata T (2002) MAFFT: a novel method for rapid multiple sequence alignment based on fast Fourier transform. Nucleic Acids Res 30(14): 3059–3066

Khonsanit A, Noisripoom W, Mongkolsamrit S, Phosrithong N, Luangsa-ard JJ (2021) Five new species of *Moelleriella* infecting scale insects (Coccidae) in Thailand. Mycol Prog 20: 847–867

Li Q, Chen C, Xiong C, Jin X, Chen Z, Huang W (2018) Comparative mitogenomics reveals large-scale gene rearrangements in the mitochondrial genome of two *Pleurotus* species. Sci Rep 102(14): 6143–6153

Li Q, Wang Q, Jin X, Chen Z, Xiong C, Li P, Liu Q, Huang W (2019) Characterization and comparative analysis of six complete mitochondrial genomes from ectomycorrhizal fungi of the *Lactarius* genus and phylogenetic analysis of the *Agaricomycetes*. Int J Biol Macromol 121: 249–260

Li Q, Xiao W, Wu P, Zhang T, Xiang P, Wu Q, Zou L, Gui M (2023) The first two mitochondrial genomes from *Apiotrichum* reveal mitochondrial evolution and different taxonomic assignment of *Trichosporonales*. IMA Fungus 14(1): 7

Li Q, Li L, Feng H, Tu W, Bao Z, Xiong C, Wang X, Qing Y, Huang W (2021) Characterization of the Complete Mitochondrial Genome of Basidiomycete Yeast *Hannaella oryzae*: Intron Evolution, Gene Rearrangement, and Its Phylogeny. Front Microbiol 12: 646567

Li Q, Li L, Zhang T, Xiang P, Wu Q, Tu W, Bao Z, Zou L, Chen C (2022) The first two mitochondrial genomes for the genus *Ramaria* reveal mitochondrial genome evolution of *Ramaria* and phylogeny of *Basidiomycota*. IMA Fungus 13(1): 16

Librado P, Rozas J (2009) DnaSP v5: a software for comprehensive analysis of DNA polymorphism data. Bioinformatics 25(11): 1451–1452

Lowe TM, Chan PP (2016) tRNAscan-SE On-line: integrating search and context for analysis of transfer RNA genes. Nucleic Acids Res 44(W1): W54–W57

Ma Q, Geng Y, Li Q, Cheng C, Zang R, Guo Y, Wu H, Xu C, Zhang M (2022) Comparative mitochondrial genome analyses reveal conserved gene arrangement but massive expansion/contraction in two closely related *Exserohilum* pathogens. Comput Struct Biotechnol J 20: 1456–1469

Mongkolsamrit S, Nguyen T, Tran NL, Luangsa-ard J (2011) *Moelleriella*

pumatensis, a new entomogenous species from Vietnam. Mycotaxon 117(1): 45–51

Mu T, Lin Y, Pu H, Keyhani NO, Dang Y, Lv H, Zhao Z, Heng Z, Wu Z, Xiong C, Lin L, Chen Y, Su H, Guan X, Qiu J (2024) Molecular phylogenetic and estimation of evolutionary divergence and biogeography of the family Schizoparmaceae and allied families (Diaporthales, Ascomycota). Mol Phylogenet Evol 201: 108221

Muñoz-Gómez SA, Wideman JG, Roger AJ, Slamovits CH (2017) The Origin of Mitochondrial Cristae from Alphaproteobacteria. Mol Biol Evol 34(4): 943–956

Murphy MP (2009) How mitochondria produce reactive oxygen species. Biochem J 417(1): 1–13

Nielsen H, Wernersson R (2016) An overabundance of phase 0 introns immediately after the start codon in eukaryotic genes. BMC Genomics 7: 256

Oborník M, Klíc M, Zizka L (2000) Genetic variability and phylogeny inferred from random amplified polymorphic DNA data reflect life strategy of entomopathogenic fungi. Can J Bot 78(9): 1150–1155

Qiu J, Song F, Mao L, Tu J, Guan X (2013) Time–dose–mortality data and modeling for the entomopathogenic fungus *Aschersonia placenta* against the whitefly *Bemisia tabaci*. Can J Microbiol 59(2): 97–101

Sadorn K, Saepua S, Punyain W, Saortep W, Choowong W, Rachtawee P,

Pittayakhajonwut P (2020) Chromanones and aryl glucoside analogs from the entomopathogenic fungus *Aschersonia confluens* BCC53152. Fitoterapia 144: 104606

Seib T, Fischer K, Sturm AM, Stephan D (2023) Investigation on the Influence of Production and Incubation Temperature on the Growth, Virulence, Germination, and Conidial Size of *Metarhizium brunneum* for Granule Development. J Fungi 9(6): 668

Slater GSC, Birney E (2005) Automated generation of heuristics for biological sequence comparison. BMC Bioinformatics 6: 31

Song X, Geng Y, Xu C, Li J, Guo Y, Shi Y, Ma Q, Li Q, Zhang M (2024) The complete mitochondrial genomes of five critical phytopathogenic *Bipolaris* species: features, evolution, and phylogeny. IMA Fungus 15(1): 15

Stone CL, Frederick RD, Tooley PW, Luster DG, Campos B, Winegar RA, Melcher U, Fletcher J, Blagden T (2018) Annotation and analysis of the mitochondrial genome of *Coniothyrium glycines*, causal agent of red leaf blotch of soybean, reveals an abundance of homing endonucleases. PLoS One 13(11): e0207062

Valach M, Burger G, Gray MW, Lang BF (2014) Widespread occurrence of organelle genome-encoded 5S rRNAs including permuted molecules. Nucleic Acids Res 42(22): 13764–13777

Wang J, Song Z, Du Y (2014) Six New Record Species of Whiteflies (Hemiptera: Aleyrodidae) Infesting *Morus alba* in China. J Insect Sci 14: 274

Wang J, Zhang L, Zhang QL, Zhou MQ, Wang XT, Yang XZ, Yuan ML (2017) Comparative mitogenomic analysis of mirid bugs (Hemiptera: Miridae) and evaluation of potential DNA barcoding markers. PeerJ 5: e3661

Wang L, Zhang S, Li J, Zhang Y (2018) Mitochondrial genome, comparative analysis and evolutionary insights into the entomopathogenic fungus *Hirsutella thompsonii*. Environ Microbiol 20(9): 3393–3405

Wang Z, Ma J, Yang Z, Jing Z, Yu Z, Li J, Yu H (2024) Morphological and Phylogenetic Analyses Reveal Three New Species of Entomopathogenic Fungi Belonging to Clavicipitaceae (Hypocreales, Ascomycota). J Fungi 10(6): 423

Wu P, Bao Z, Tu W, Li L, Xiong C, Jin X, Li P, Gui M, Huang W, Li Q (2021) The mitogenomes of two saprophytic Boletales species (*Coniophora*) reveals intron dynamics and accumulation of plasmid-derived and non-conserved genes. Comput Struct Biotechnol J 19: 401–414

Xia Y, Zheng Y, Murphy RW, Zeng X (2016) Intraspecific rearrangement of mitochondrial genome suggests the prevalence of the tandem duplication-random loss (TDLR) mechanism in *Quasipaa boulengeri*. BMC Genomics 17(1): 965

Xiang CY, Gao F, Jakovlić I, Lei HP, Hu Y, Zhang H, Zou H, Wang GT, Zhang D (2023) Using PhyloSuite for molecular phylogeny and tree - based analyses. iMeta 2(1): e87

Yang Z, Wang Z, Ma J, Yu H (2023) *Moelleriella simaoensis*, a new

entomogenous species of *Moelleriella* (Clavicipitaceae, Hypocreales) from Southwestern China. Phytotaxa 603: 60–68

Zhang YJ, Fan XP, Li JN, Zhang S (2013) Mitochondrial genome of *Cordyceps blackwelliae*: organization, transcription, and evolutionary insights into *Cordyceps*. IMA Fungus 14(1): 13

Zhao Z, Mu T, Keyhani NO, Pu H, Lin Y, Lv Z, Xiong J, Chen X, Zhan X, Lv H, Jibola-Shittu MY, Jia P, Wu J, Huang S, Qiu J, Guan X (2024) Diversity and New Species of Ascomycota from Bamboo in China. J Fungi 10(7): 454

Zheng BY, Cao LJ, Tang P, van Achterberg K, Hoffmann AA, Chen HY, Chen XX, Wei SJ (2018) Gene arrangement and sequence of mitochondrial genomes yield insights into the phylogeny and evolution of bees and sphecid wasps (Hymenoptera: Apoidea). Mol Phylogenet Evol 124: 1–9

Zhu Z, Zhuang W (2015) *Trichoderma* (*Hypocrea*) species with green ascospores from China. Persoonia 34: 113–129

Zubaer A, Wai A, Patel N, Perillo J, Hausner G (2021) The Mitogenomes of *Ophiostoma minus* and *Ophiostoma piliferum* and Comparisons With Other Members of the Ophiostomatales. Front Microbiol 12: 618649

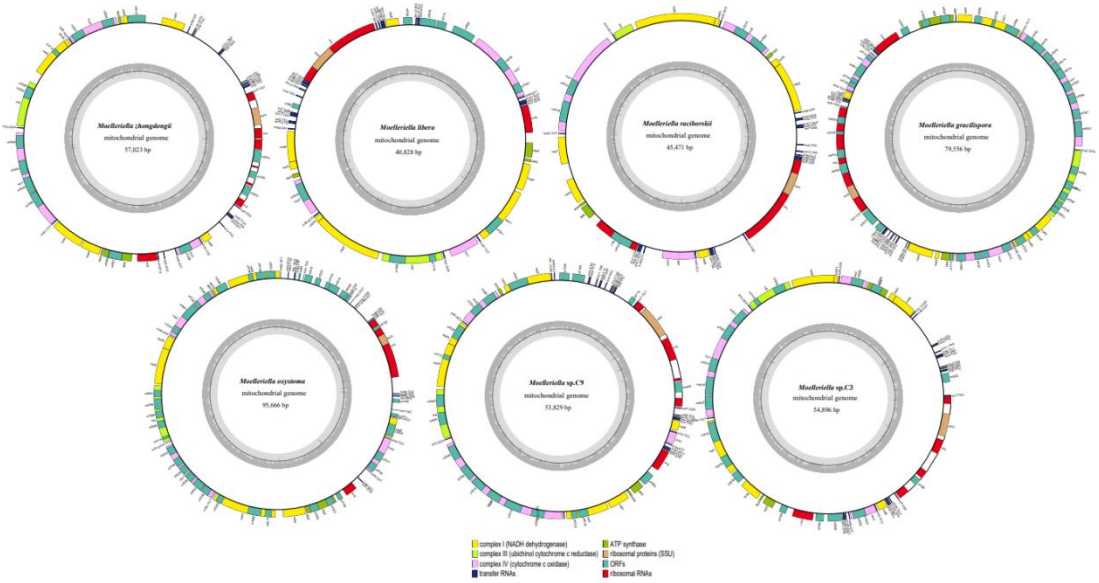

Fig. 1. Circular maps of the mitochondrial genomes of seven *Moelleriella* species. Genes are represented by different coloured blocks. All functional genes were in the same strand. Gray plot in the inner circle indicates GC content.

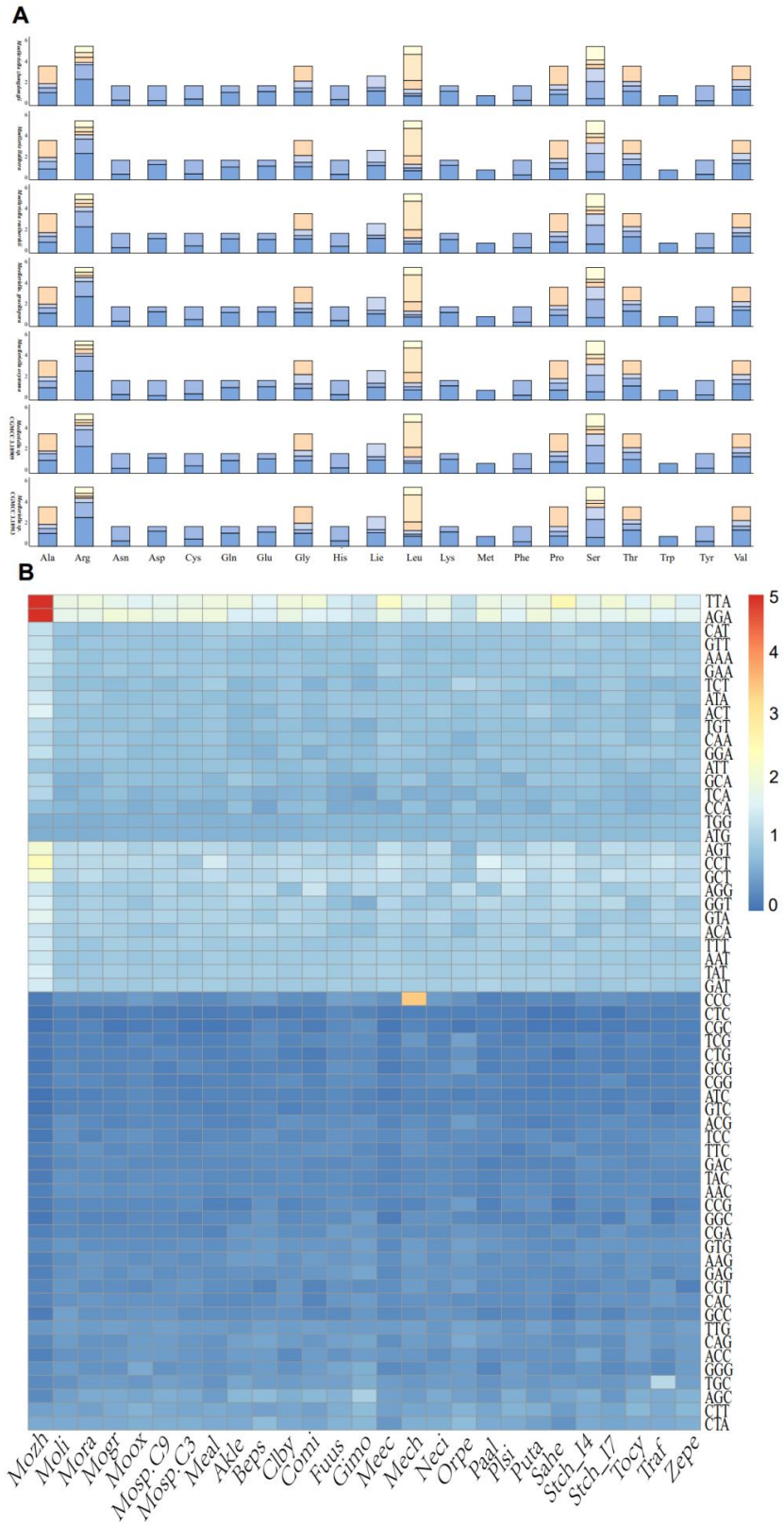

Fig. 2. (A) Stacked column plots of the Relative Synonymous Codon Usage (RSCU) of the seven *Moelleriella* mitogenomes. (B) Heatmap of the RSCU of the mitogenomes of 27 Hypocreales species.

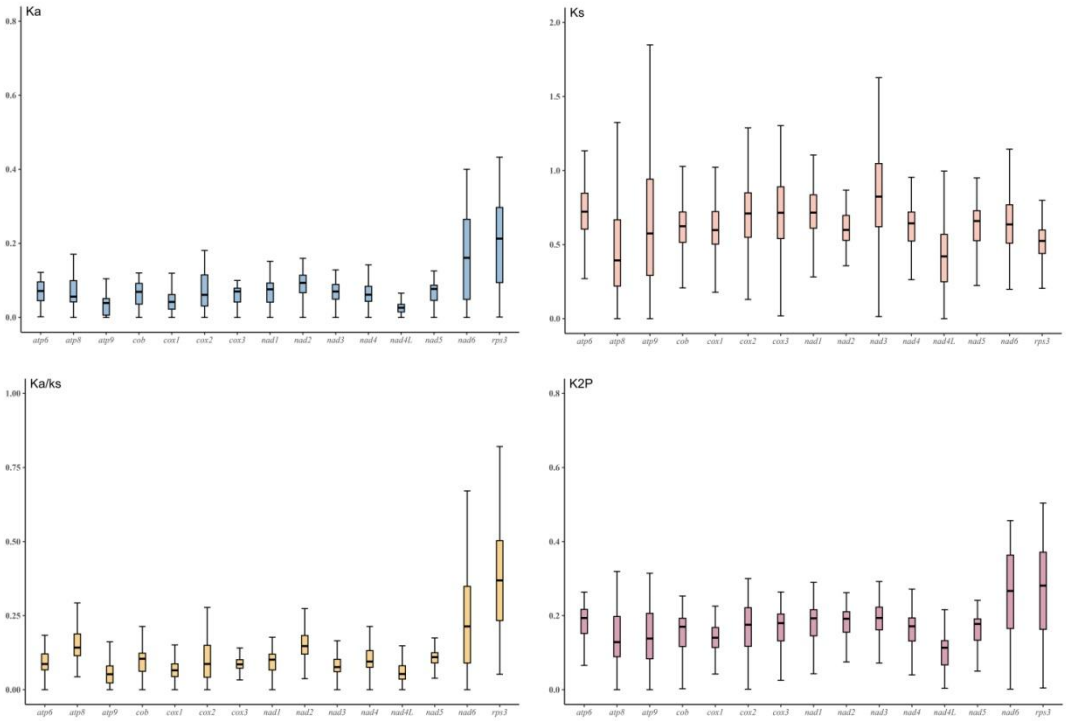

Fig.3. Genetic analysis of the 15 protein-coding genes (PCGs) conserved in the 27 Hypocreales mitogenomes. K2P, the Kimura-2-parameter distance; Ka, the mean number of nonsynonymous substitutions per nonsynonymous site; Ks, the mean number of synonymous substitutions per synonymous site.

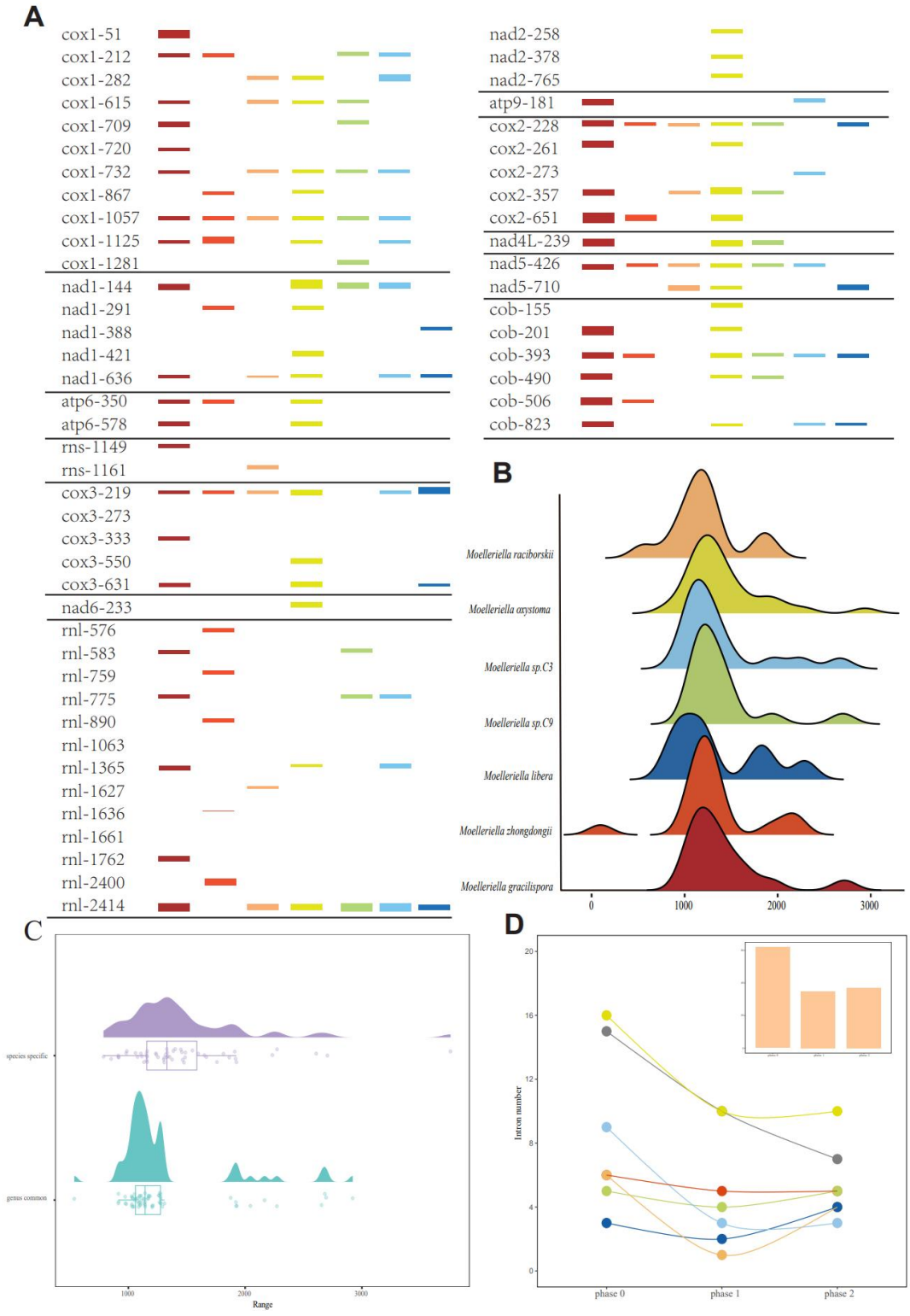

Fig. 4. Intron position sets (IPSs) in mitogenomes of the genus *Moelleriella* and Characteristics of the introns of *Moelleriella* species. (A)Bar graph indicating intron dynamics among seven *Moelleriella* species. Intron insertion positions were referred to coding sequences of the *M. gracilispora* genes. The height of each bar corresponded to its

respective intron length. (B)The length distribution of the total introns of the *Moelleriella* species. (C)Box plots indicating length distributions of common introns and species-specific introns, respectively. (D)Codon phase distributions of intron insertion position.

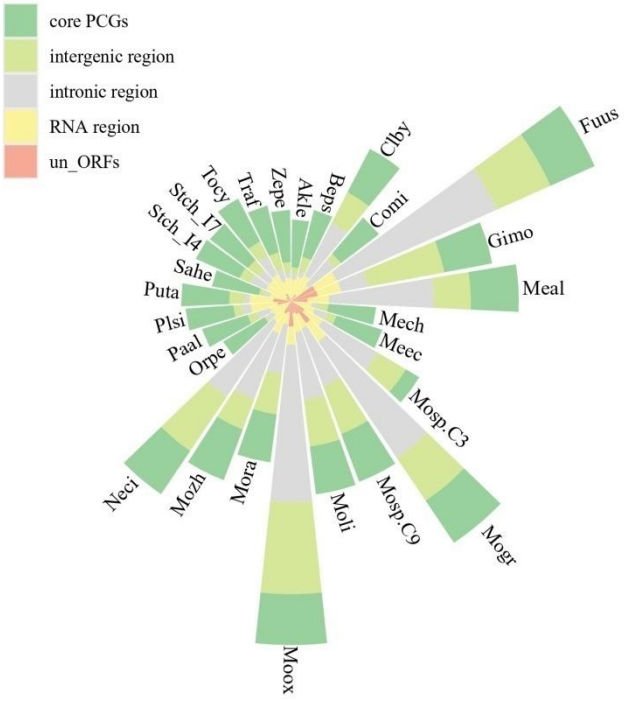

Fig. 5. The lengths of RNA region, core PCGs, intronic region, un_ORFs, and intergenic region in 27 Hypocreales species.

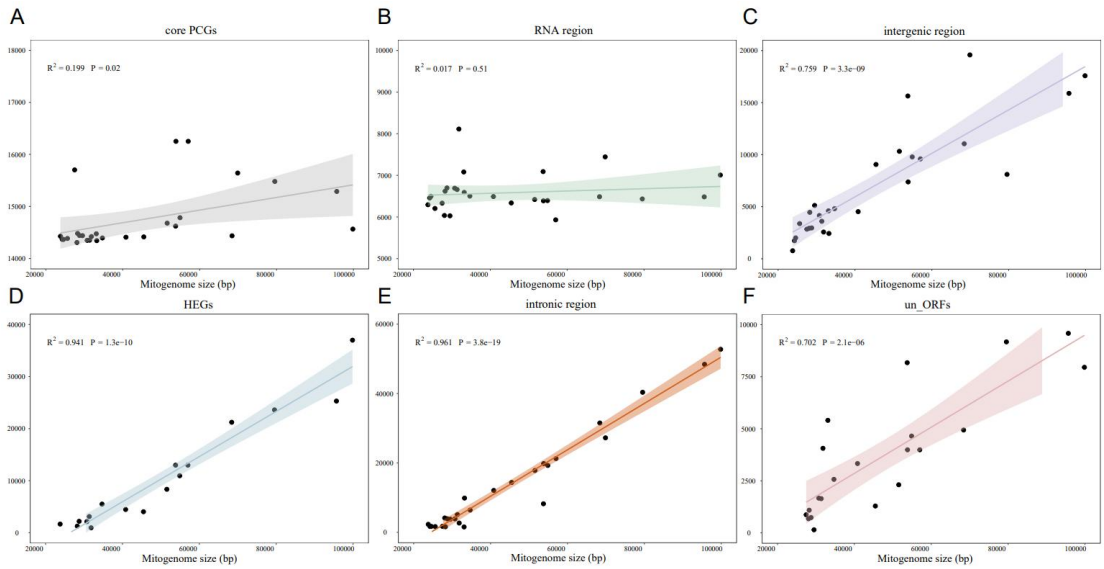

Fig. 6. Correlation analysis between the lengths of mitogenomes and the lengths of (A)core PCGs(B), intergenic region (C), HEGs (D), RNA region (E), intronic region, (F)un_orf.

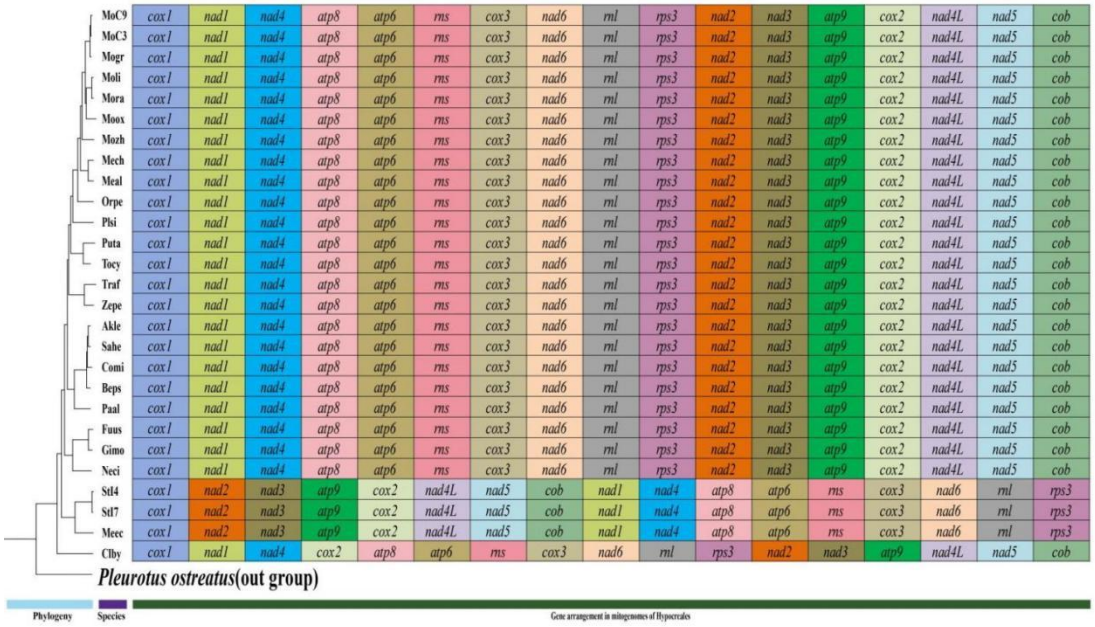

Fig. 7. Gene order analyses for 27 Hypocreales mitogenomes. The same gene is represented by the same background color. All genes (fifteen core PCGs and two ribosomal RNAs) are shown in the order of their appearance in the mitogenome, starting with *cox*1.

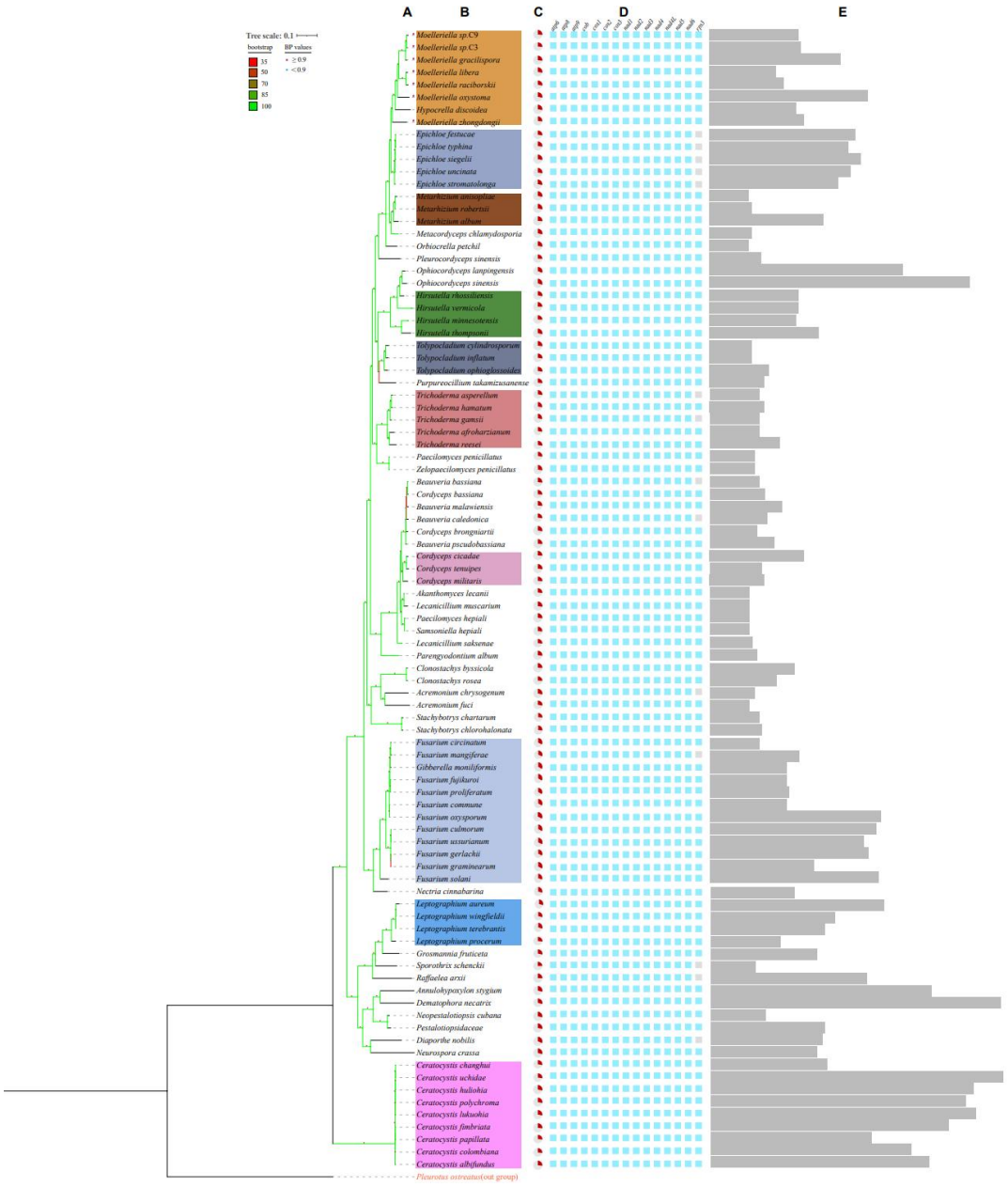

Fig. 8. A phylogenetic tree inferred from concatenated mitogenomic PCGs of 94 Ascomycota species, based on Bayesian inference (BI) and Maximum likelihood (ML) methods. (A, B) Tree topology and species list showing the branching of lineages. The bootstrap values of tree nodes were colour coded. Nodes marked red and blue points indicated Bayesian posteriors probability (BP) values equal [0.9, 1] and <0.9, respectively. Genera containing $\geqslant 3$ species were filled with the same colours in the species list. (C) GC contents (D) Checkmark indicating related species had fungal standard

PCGs altogether. (E) genome sizes of corresponding mitogenomes.

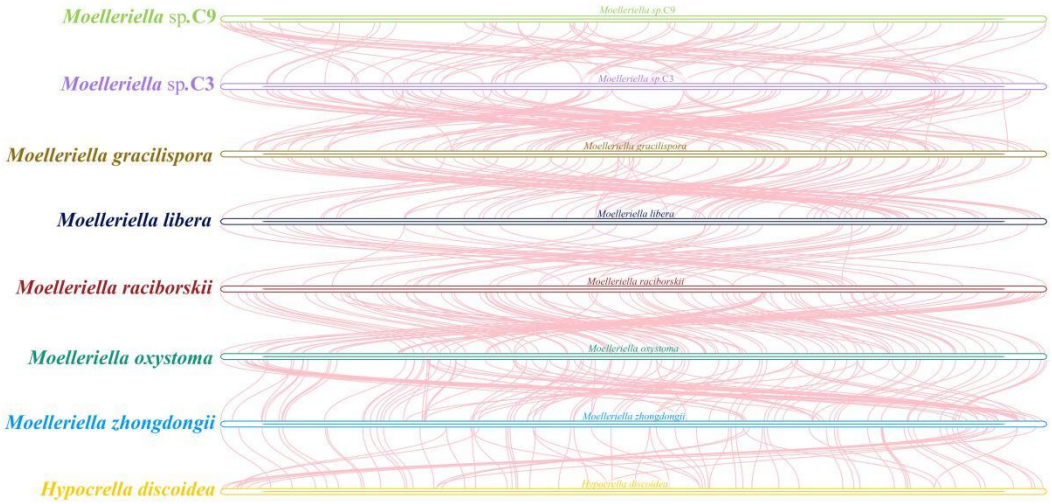

Fig. 9. *Moelleriella* mitogenomes synteny. Bars indicate mitogenomes and red regions indicate regions of covariance.